

Sterile Neutrino Searches with MicroBooNE: Electron Neutrino Disappearance

Peter B. Denton*

*High Energy Theory Group, Physics Department,
Brookhaven National Laboratory, Upton, NY 11973, USA*

A sterile neutrino is a well motivated minimal new physics model that leave an imprint in neutrino oscillations. Over the last two decades, a number of hints pointing to a sterile neutrino have emerged, many of which are pointing near $m_4 \sim 1$ eV. Here we show how MicroBooNE data can be used to search for electron neutrino disappearance using each of their four analysis channels. We find a tantalizing hint for oscillations with the highest single channel significance of 2.2σ (assuming Wilks' theorem) coming from the Wire-Cell analysis which prefers $\sin^2(2\theta_{14}) = 0.30$ and $\Delta m_{41}^2 = 1.42$ eV²; the other partially independent channels have compatible hints. This region of parameter space is in good agreement with existing hints from source experiments, is at a similar frequency but higher mixing than indicated by reactor anti-neutrinos, and is at the edge of the region allowed by solar neutrino data. Existing unanalyzed data from MicroBooNE could increase the sensitivity to 2.8σ and future data can reach $> 3\sigma$ with existing systematics, assuming Wilks' theorem.

I. INTRODUCTION

Sterile neutrino searches have played a major part of new physics searches in the neutrino sector, and with good reason. Given that neutrinos have mass, it is highly anticipated that sterile neutrinos exist with some mixing with the active neutrinos. This parameter space for the mixings and the masses for sterile neutrinos, however, spans many orders of magnitude [1] and no guaranteed prediction exists encouraging a broad search program.

Due to a variety of hints of sterile neutrinos at the $m_4 \sim 1$ eV scale from LSND, the reactor anti-neutrino anomaly (RAA), the gallium anomaly, and the Mini-BooNE anomaly [2–6], an intense global effort to understand these hints has accelerated in recent years; for recent reviews see [7–9]. The various oscillation probes of $m_4 \sim 1$ eV sterile neutrinos can be generally classified into three dominant categories: 1) ν_e disappearance containing solar, reactor, and source calibration data, 2) ν_μ disappearance containing accelerator and atmospheric data, and 3) $\nu_\mu \rightarrow \nu_e$ appearance data containing accelerator data. Thus far hints exist in ν_e disappearance [3–5] and $\nu_\mu \rightarrow \nu_e$ appearance [2, 6] but no significant evidence for new oscillation frequencies has been seen in ν_μ disappearance [10, 11]. Since $\nu_\mu \rightarrow \nu_e$ appearance requires both ν_e disappearance and ν_μ disappearance with the same frequency and partially constrained mixing angles, the evidence for $\nu_\mu \rightarrow \nu_e$ appearance has been considered to be in tension with the lack of evidence for steriles from ν_μ disappearance, see e.g. [12].

At higher masses, a low significance hint of a sterile neutrino mixing with electron neutrinos exists in tritium data from KATRIN at $\Delta m_{41}^2 \sim 300$ eV² [13, 14]. At further higher masses, sterile neutrinos in the keV range could be related to dark matter [15] and there may already be hints of such particles [16, 17], although these hints are still being investigated [18–25]. Finally, strong

constraints from cosmological measurements of the Cosmic Microwave Background and Baryon Acoustic Oscillations exist [26] although the Hubble tension [27, 28] may be pointing to evidence for a new degree of freedom in the early universe [29]. These constraints could also be partially alleviated in new physics models, typically with a new low scale interaction [30–37].

Recently MicroBooNE reported their first search for ν_e events with 7×10^{20} POT in a dominantly ν_μ beam to test MiniBooNE's evidence for ν_e appearance. Their data was analyzed in four different analysis channels with different final state cuts. They did not see electron neutrinos at the rate predicted by MiniBooNE [38–41] and disfavored ν_e appearance consistent with MiniBooNE's excess at 3.75σ in the most sensitive analysis [41]. Additionally, the next two most sensitive analyses also disfavored the rate predicted by MiniBooNE [39, 40] at lesser significance, and only the least sensitive channel found an excess of ν_e events over the background, but at low $< 1\sigma$ evidence [40].

There is more information in MicroBooNE data than just a constraint on $\nu_\mu \rightarrow \nu_e$ appearance. Due to the presence of intrinsic ν_e in the beam, we will show that MicroBooNE has not only modest sensitivity to ν_e disappearance searches, but also interesting hints for ν_e disappearance, compatible with many of the existing data sets in the literature, including some hints in the same regions of parameter space. This hint can be further tested as the whole three detector short-baseline neutrino program at Fermilab comes online. This program benefits from many shared systematics, all of which are quite independent from those in reactor, solar, and source searches.

MiniBooNE also sat in a similar accelerator beam and thus one could imagine looking for evidence of ν_e disappearance in their data, however their backgrounds from π^0 misidentification, $\Delta \rightarrow N\gamma$, and others dominated over ν_e events, while the opposite is true for MicroBooNE due to the awesome reconstruction power of Liquid Argon Time Projection Chambers (LArTPCs). In addition, MiniBooNE has reported an excess of electron neutrino candidate events [6] which seem to require an explanation

* pdenton@bnl.gov; 0000-0002-5209-872X

beyond a $m_4 \sim 1$ eV sterile neutrino due to constraints from MicroBooNE, MINOS+, IceCube, and cosmology [10, 11, 26, 38–41], some of which could potentially be evaded in more complicated models [29–37, 42, 43]. It is still to be determined if existing explanations of Mini-BooNE without a $m_4 \sim 1$ eV sterile neutrino [44–54] are also consistent with MicroBooNE’s new results.

In this article we will present the sterile neutrino oscillation analysis of the MicroBooNE data focusing on the Wire-Cell analysis in section II; the analysis of the other three channels and the comparison of all four can be found in the appendix. Next, we will compare the MicroBooNE results to others in the literature in section III. We then discuss our results and conclude in section IV and V. All the data files associated the parameter scans shown in figs. 2, 7, and 8 can be found at peterdenton.github.io/Data/Micro_Dis/index.html.

II. ANALYSIS

MicroBooNE has reported four separate analyses dubbed Wire-Cell [41] which is sensitive to final states with one electron and anything else, Pandora [40] which is sensitive to final states with one electron, zero pions, and either zero protons or 1+ protons, and Deep-Learning [39] which is sensitive to final states with one electron and one proton in a charged-current quasi-elastic interactions. Each of these four analyses has different strengths and weaknesses in terms of statistics, purity, and calibration data and are summarized in [38]. As the Wire-Cell analysis has the highest sensitivity to Mini-BooNE’s electron neutrino appearance signal and the highest statistics, we take it as our fiducial analysis, but we also investigate the other channels for completeness, see the appendix.

To analyze the MicroBooNE data in terms of a sterile neutrino, we consider a two parameter model where the sterile neutrino mixes only with electron neutrinos. Thus the expected ν_e events will be reduced by the disappearance probability

$$P(\nu_e \rightarrow \nu_e) = 1 - \sin^2(2\theta_{14}) \sin^2\left(\frac{\Delta m_{41}^2 L}{4E}\right), \quad (1)$$

where $L = 470$ m is MicroBooNE baseline [55], $\Delta m_{41}^2 \equiv m_4^2 - m_1^2$ is the new oscillation frequency, and θ_{14} gives the amplitude of the oscillations.

While a full analysis including a combination of all channels, a full treatment of energy reconstruction, backgrounds, and other systematics along with a Feldman-Cousins [56] parameter scan is necessary to robustly quantify the statistical significance of these sterile oscillations, we can still get a good estimate of the parameters of interest preferred in a simplified analysis. In order to quantify the significance we will assume Wilks’ theorem

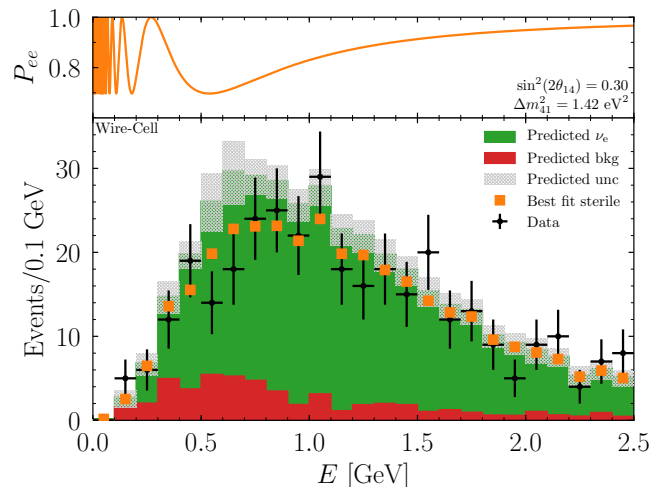


FIG. 1. **Top:** The disappearance probability for the best fit set of sterile oscillation parameters, $\Delta m_{41}^2 = 1.42$ eV² and $\sin^2(2\theta_{14}) = 0.30$, for the Wire-Cell data. **Bottom:** The expected event rate at MicroBooNE in the Wire-Cell analysis [41] including contributions from backgrounds (red) and ν_e events (green) along with the theory uncertainty (gray hatched). The actual data is shown in black and the expected data rate, assuming the best fit sterile hypothesis, is shown in orange.

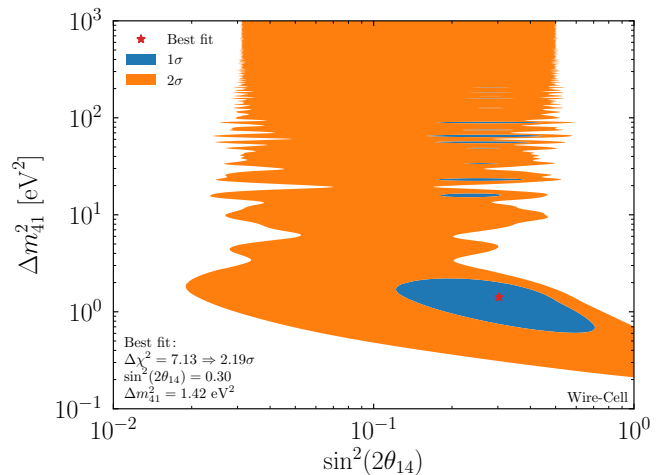


FIG. 2. The preferred regions in $\Delta m_{41}^2 - \sin^2(2\theta_{14})$ parameter space using data from MicroBooNE’s Wire-Cell analysis [41]. The blue (orange) region is the preferred region at 1σ (2σ) assuming Wilks’ theorem. The red star is at the best fit point: $\Delta m_{41}^2 = 1.42$ eV² and $\sin^2(2\theta_{14}) = 0.30$ which has a test statistic of $\Delta\chi^2 = 7.13$ to no oscillations which implies 2.19σ under Wilks’ theorem.

and use a test statistic,

$$\chi^2(\Delta m_{41}^2, \sin^2(2\theta_{14})) = \sum_i \frac{(N_{\text{data},i} - N_{\text{pred,bkg},i} - N_{\text{pred},\nu_e,i} \bar{P}_{ee})^2}{N_{\text{pred,total},i} + \sigma_{\text{th},i}^2}, \quad (2)$$

where the sum goes over the energy bins in the analysis, $N_{\text{data},i}$ is the number of recorded events in bin i , $N_{\text{pred,bkg},i}$ is the number of expected non- ν_e events in bin i , $N_{\text{pred},\nu_e,i}$ is the number of expected ν_e events in bin i , $N_{\text{pred,total},i} \equiv N_{\text{pred,bkg},i} + N_{\text{pred},\nu_e,i}$, and \bar{P}_{ee} is the disappearance probability averaged over bin i . Finally, the theory uncertainty on the prediction in bin i is $\sigma_{\text{th},i}$. For the Wire-Cell (Pandora-Np) analysis we start with the $[0.1, 0.2]$ ($[0.14, 0.28]$) GeV bin as the statistics in the lowest energy bin are essentially zero in these two analyses.

In fig. 1 we show the contributions to the predicted spectra and its theory uncertainty, the data, and the expected data given the best fit sterile neutrino point, along with the sterile neutrino oscillation probability at the best fit point. To determine the best fit point in sterile neutrino parameter space, we performed a scan, shown in fig. 2, showing contours of the test statistic that correspond to $1, 2\sigma$ assuming Wilks' theorem. The results for the other three analysis channels are shown in the appendix.

III. PREVIOUS ν_e DISAPPEARANCE PROBES

Existing probes of light sterile neutrinos mixing with ν_e 's exist from gallium data, reactor data, and solar data. We show the preferred regions (disfavored region in the case of solar) for all of these data from [5, 57, 58] in fig. 3. Existing hints for a sterile neutrino from gallium data collected by SAGE, GALLEX, and BEST [5, 59, 60] show a high significance preference for sterile parameters consistent with that from MicroBooNE. There exist various interpretations of the gallium anomalies with different theory estimates and, while the significances vary from $\sim 2.3\sigma$ to $> 3\sigma$ with the latest BEST data, the central values and thus preferred regions remain similar in the analyses [5, 61, 62].

Reactor anti-neutrino data has received considerable attention in the last decade. A recent analysis of modern reactor data [57] finds a preference for oscillations at $\Delta m_{41}^2 = 1.26 \text{ eV}^2$, consistent with this MicroBooNE analysis, but with a smaller mixing angle. The significance of the reactor data is under intense scrutiny with different estimates of the significance for oscillations varying from $\lesssim 1\sigma$ to 3.2σ and the impact of fuel evolution studies may partially weaken the evidence for sterile neutrinos in reactor data but seems to not remove it completely [57, 63–70]. In addition, while some reactor flux predictions, in particular [71–73] are compatible with the MicroBooNE hint; others such as [66, 74, 75] provide a constraint slightly weaker than that from solar for $\Delta m_{41}^2 \gtrsim 1 \text{ eV}^2$ in slight tension with the MicroBooNE and gallium hints; see [66] for a comparison of the different reactor predictions.

It is also possible to probe the existence of a sterile neutrino indirectly through an analysis looking for evidence of unitary violation of the lepton mixing matrix. Vari-

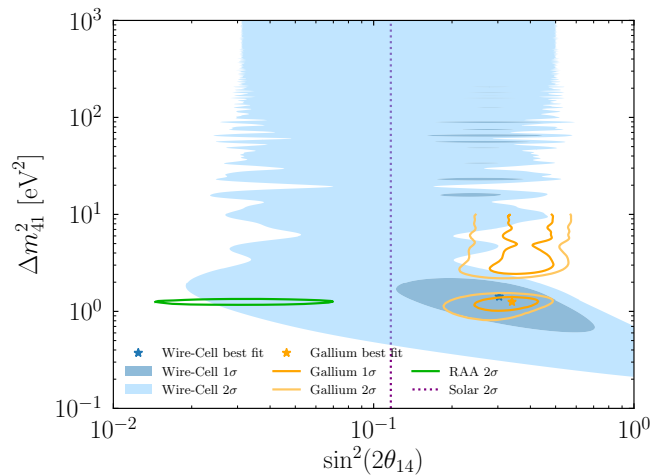


FIG. 3. The preferred regions from MicroBooNE’s Wire-Cell analysis [41] as calculated in this paper (blue), from BEST [5] combined with other gallium data from SAGE [59] and GALLEX [60] (orange), and a global analysis of modern reactor anti-neutrino data [57] (green). Additionally, solar neutrinos disfavor large mixing angles [58] (purple).

ous analyses have drawn rather tight constraints on such mixing from observing that the three dominant terms in the electron row $|U_{e1}|^2 + |U_{e2}|^2 + |U_{e3}|^2$ seem to sum very close to one at the few percent to per mille level [76–78]. Care is required, however, as these analyses avoid any data sets that show evidence for violation of unitarity in the standard three flavor oscillation picture from e.g. LSND, MiniBooNE, RAA, or gallium experiments.

IV. DISCUSSION

A combined analysis of the four different channels would likely increase the significance for a sterile neutrino as the data sets are not entirely independent, see fig. 8 and table II in the appendix. Moreover, due to many shared systematics with regards to flux, cross sections, and detector performance, there should be a partial cancellation of the theory uncertainties. Considerable care is required, however, as such a combined analysis would require intimate knowledge of the experiment, as well as all of the individual analyses which is beyond the scope of this paper. Nonetheless, we see that there is general agreement, among the different analyses, that the data indicates oscillations at $\Delta m_{41}^2 \sim 1.5 \text{ eV}^2$ and $\sin^2(2\theta_{14}) \gtrsim 0.1$.

In this analysis, we assumed that the backgrounds would be unmodified by the presence of a sterile neutrino but, neutral current (NC) events provide an considerable contribution to the backgrounds in the Wire-Cell analysis and a sterile neutrino would deplete this contribution. This contribution is safely ignored in this analysis since a) the backgrounds are quite small compared to the neutrino signal in this analysis and the NC

events are a subset of those implying a modification due to sterile neutrinos would be quite minor and b) the neutrino flux at MicroBooNE is expected to be dominantly ν_μ and since we are considering a sterile neutrino that mixes only with ν_e ; the ν_μ contribution to the NC flux would be unaffected.

The preferred region shown in fig. 2 that continues to large values of Δm_{41}^2 is in the oscillation averaged regime and is independent of Δm_{41}^2 . This region is preferred due to the overall deficit in ν_e candidate events. At lower values of $\Delta m_{41}^2 \lesssim 0.5 \text{ eV}^2$ the oscillations do not have enough time to materialize before reaching MicroBooNE.

Unlike other hints and probes of light sterile neutrinos, MicroBooNE's hint is in the central region of their spectrum showing signs of an oscillation minimum. Other probes depend on a total rate measurement (medium-baseline reactor, solar, and source experiments) or the only signal that is seen is at the edge of the energy spectrum (short-baseline accelerator appearance searches at LSND and MiniBooNE)¹. For example, for the best fit oscillation parameters in the Wire-Cell analysis, the oscillation minimum is at $E \sim 0.5 \text{ GeV}$. While somewhat on the lower energy end of their spectrum, there are still modest statistics below that point. Similar results are true for the other analysis channels although the statistics in the Pandora-0p analysis are quite low. This provides an important robustness test as experimental or other new physics effects are unlikely to materialize as a deficit of events localized in a certain energy range.

In the future, this sterile neutrino hint can be tested at a range of experiments including MicroBooNE as more data is accumulated. In fact, MicroBooNE has already accumulated 12×10^{20} POT, almost a factor of two above what is presented in this analysis. The expected sensitivity for the best fit point in this analysis and a benchmark point from reactor neutrinos is shown in fig. 4 which shows that with existing data the significance would be at the 2.8σ level and MicroBooNE's Wire-Cell analysis alone can reach $> 3\sigma$ as further data accumulates with existing theory uncertainties, up to corrections from Feldman-Cousins. The preferred value from reactor anti-neutrinos, $\Delta m_{41}^2 = 1.25 \text{ eV}^2$ and $\sin^2(2\theta_{14}) = 0.032$ [57], has too small of a mixing to be tested at MicroBooNE; a significant improvement in the systematics and the full short-baseline neutrino program could change this.

In addition, the short baseline neutrino program at Fermilab with three similar LArTPC detectors at different baselines in the same neutrino beam [55] can test this scenario with considerable cancellation of systemat-

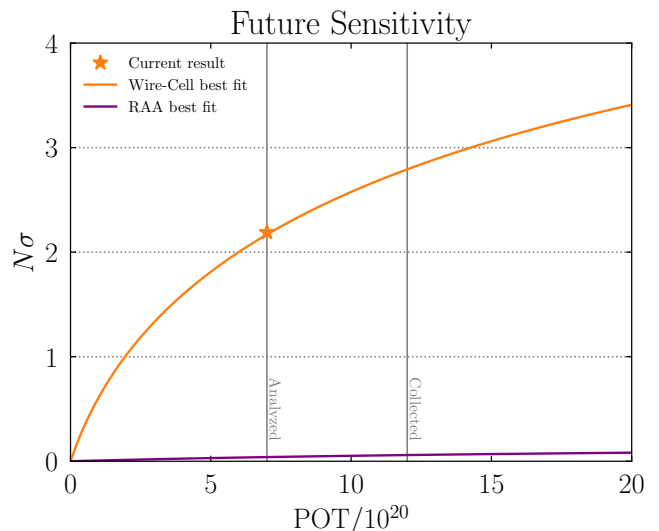


FIG. 4. The projected sensitivity in numbers of standard deviations assuming Wilks' theorem with two degrees of freedom as a function of POT. The sensitivity to the best fit point from MicroBooNE's Wire-Cell analysis is shown in orange. The orange star represents the results from this analysis indicating that the data is not experiencing large fluctuations relative to the best fit sterile hypothesis. The purple curve is the projected sensitivity to the best fit reactor anti-neutrino point, $\Delta m_{41}^2 = 1.25 \text{ eV}^2$ and $\sin^2(2\theta_{14}) = 0.032$ [57].

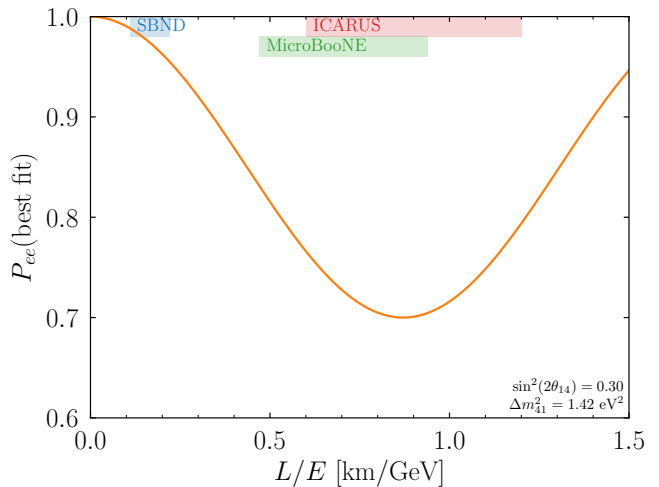


FIG. 5. The disappearance probability for the best fit oscillation parameters along with the primary kinematic range of each of the three detectors in the short baseline neutrino program at Fermilab.

¹ Two exceptions are short-baseline reactor experiments and IceCube [11] in their ν_μ disappearance search which is expected to see no significant oscillations at the edge of their spectrum and for neutrinos traveling shorter distances through the Earth and a larger deficit of ν_μ 's in the middle of their energy range for up-going neutrinos. IceCube, however, is not sensitive to sterile neutrinos mixing with ν_e 's.

ics due to the presence of the same flux and same target nuclei at different baselines. The best fit oscillation probability and the kinematic range probed by the three detectors are shown in fig. 5. If a sterile neutrino exists with these parameters, the short baseline near detector (SBND) will see a nearly un-oscillated flux, MicroBooNE has observed a deficit in the lower energy portion of their

spectrum, and ICARUS will see a deficit in the higher energy part of their spectrum. In addition, it is vital to continue theory work on understanding the fluxes, cross sections, and data sets for reactor, source, and solar experiments.

V. CONCLUSIONS

While hailed as a ν_e appearance experiment, MicroBooNE, due to the spectacular particle identification power of LArTPCs, can identify the intrinsic ν_e component of the flux. We have shown that it is possible to use this flux to probe neutrino oscillations and, in fact, we find hints for sterile oscillations in all four analysis channels presented by MicroBooNE with significances from $> 1\sigma$ to $> 2\sigma$. These hints are generally compatible with each other and come from data sets that are partially independent. Extremely tantalizing is the $> 3\sigma$ hint for sterile neutrino oscillations from a combined analysis of SAGE, GALLEX, and BEST data for the same parameters.

A sterile neutrino with $m_4 \sim 1$ eV is in modest tension however, with reactor and solar data, and is in considerable tension with cosmological measurements. Cosmological constraints on light sterile neutrinos may be partially alleviated in more involved new physics scenarios such as those with new interactions and may actually partially resolve the Hubble tension.

Looking to the future, a joint fit of each analysis channel would be expected to increase the significance beyond the 2.2σ (assuming Wilks' theorem) from the Wire-Cell analysis as more channels at MicroBooNE are investigated and more data is analyzed, if this is a sterile neutrino. In addition, the two upcoming detectors of Fermilab's short-baseline neutrino program, SBND and ICARUS, are well positioned to further probe this hint.

It is premature to conclude that MicroBooNE has killed light sterile neutrinos when, in fact, their data is pointing towards them.

ACKNOWLEDGMENTS

We acknowledge support from the US Department of Energy under Grant Contract DE-SC0012704. The figures were done with `python` [79] and `matplotlib` [80].

Appendix A: Other MicroBooNE analyses

We repeat the analysis presented in section II for the other three analysis channels: Deep-Learning, Pandora with 1+ protons, and Pandora with 0 protons. The results are visually presented in figs. 6 and 7. In addition,

the preferred sterile oscillation parameters at 1σ from all four analyses are simultaneously shown in fig. 8. Numer-

TABLE I. The best fit parameters, the test statistic between the best fit point and the no oscillation hypothesis, and the implied significance of the evidence for oscillations assuming Wilks' theorem. Note that the preferred regions have a number of degeneracies as is typical for oscillation searches thus some care is required when looking at the best fit points, see figs. 2 and 7.

Analysis	$\sin^2(2\theta_{14})$	Δm_{41}^2 (eV ²)	$\Delta\chi^2$	$N\sigma$
Wire-Cell	0.30	1.42	7.13	2.19
Deep-Learning	0.79	3.87	3.63	1.40
Pandora-Np	0.66	9.12	6.78	2.12
Pandora-0p	0.88	1.85	2.59	1.09

ically, the best fit points and significances are shown in table I.

The Pandora pipeline presents an analysis where the ν_e prediction is constrained with high purity ν_μ data. We take the ν_e and background rates from the unconstrained analysis and the theory uncertainty from the constrained analysis. We do this because the constrained analysis allows for a more robust analysis of the theory uncertainty and the unconstrained predictions are lower and thus result in conservative estimates of the significance. This difference only applies to the Np analysis as the constrained and unconstrained total background predictions for the 0p analysis are nearly equivalent.

We see in fig. 8 that three of the four analyses have overlap in the $\Delta m_{41}^2 \in [1, 2]$ eV² range while the lowest Δm_{41}^2 island from the Deep-Learning analysis is a bit higher in the $[3, 4]$ eV² range. We also note that, while the Pandora-Np analysis prefers Δm_{41}^2 close to 10 eV² due to the over-fluctuation in the $E = 0.9$ GeV bin, they still find a good fit in the same $[1, 2]$ eV² range as in the Wire-Cell and Pandora-0p analyses.

We also show the matrix of overlapping events in the different analyses in table II. We see, for example, that $\gtrsim 90\%$ of the events that appear in the Wire-Cell analysis are unique to that analysis, while 70% of the events in the Pandora-Np analysis are also in the Wire-Cell analysis. In addition, 80% of the events in the Pandora-0p analysis are unique to that analysis and the only overlap of those events with other analyses is with 1% of the Wire-Cell events. Finally, the events in Deep-Learning analysis have significant overlap with the Wire-Cell and Pandora-Np analyses. Thus while these data sets are certainly not independent and the two most significant analyses (Wire-Cell and Pandora-Np) have significant overlap, the Pandora-0p analysis is fairly independent of Wire-Cell and completely independent (statistics wise) of the other two analyses.

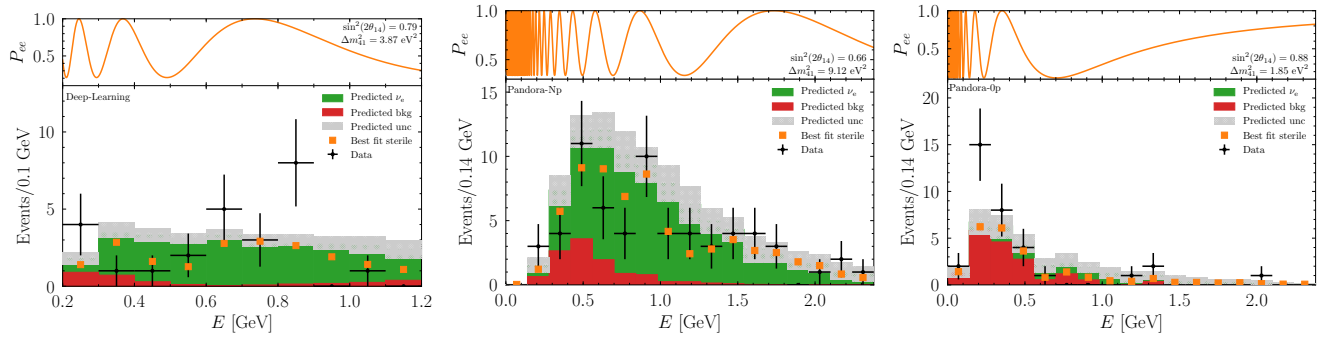


FIG. 6. The same as fig. 1 but with data from MicroBooNE’s Deep-Learning analysis (**left**) [39], the Pandora analysis with 1+ protons (**middle**), and the Pandora analysis with 0 protons (**right**) [40].

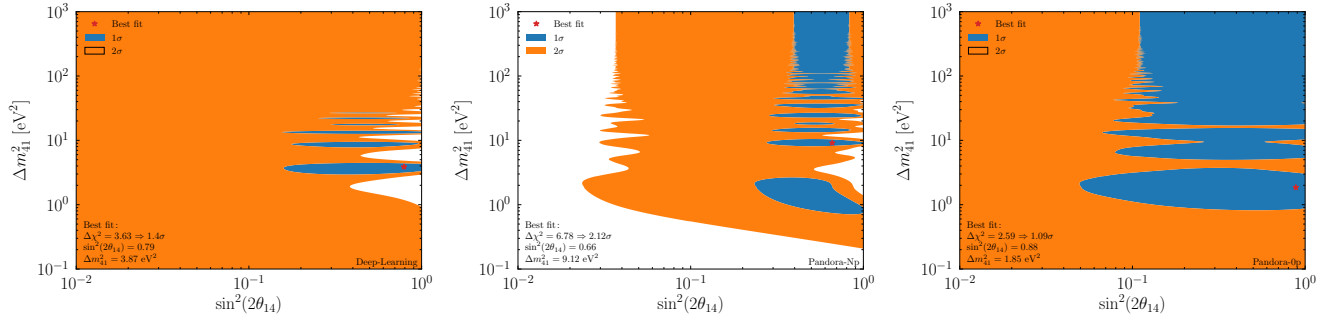


FIG. 7. The same as fig. 2 but with data from MicroBooNE’s Deep-Learning analysis (**left**) [39], the Pandora analysis with 1+ protons (**middle**), and the Pandora analysis with 0 protons (**right**) [40].

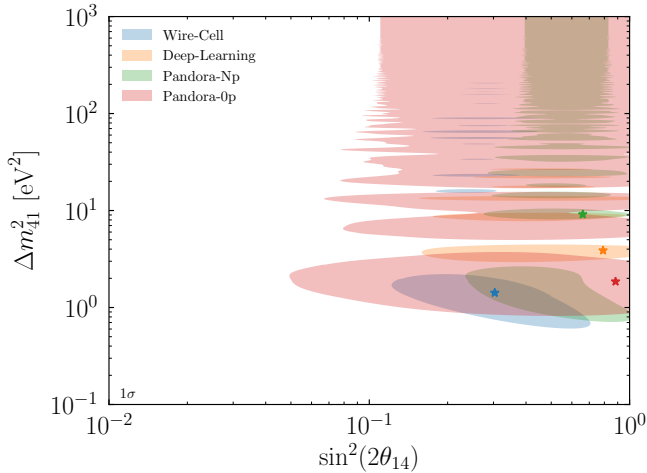


FIG. 8. The preferred regions of parameter space at 1σ from each of the four MicroBooNE analyses.

TABLE II. The number of events in the four MicroBooNE analyses that appear in multiple analyses, from [81].

Analysis	W-C	D-L	Pan-Np	Pan-0p
Wire-Cell	606	15	45	7
Deep-Learning	15	25	9	0
Pandora-Np	45	9	64	0
Pandora-Op	7	0	0	35

- [1] P. D. Bolton, F. F. Deppisch, and P. S. Bhupal Dev, *JHEP* **03**, 170 (2020), arXiv:1912.03058 [hep-ph].
- [2] A. Aguilar-Arevalo *et al.* (LSND), *Phys. Rev. D* **64**, 112007 (2001), arXiv:hep-ex/0104049.
- [3] G. Mention, M. Fechner, T. Lasserre, T. A. Mueller, D. Lhuillier, M. Cribier, and A. Letourneau, *Phys. Rev. D* **83**, 073006 (2011), arXiv:1101.2755 [hep-ex].
- [4] C. Giunti and M. Laveder, *Phys. Rev. C* **83**, 065504 (2011), arXiv:1006.3244 [hep-ph].
- [5] V. V. Barinov *et al.*, (2021), arXiv:2109.11482 [nucl-ex].
- [6] A. A. Aguilar-Arevalo *et al.* (MiniBooNE), *Phys. Rev. D* **103**, 052002 (2021), arXiv:2006.16883 [hep-ex].
- [7] P. A. Machado, O. Palamara, and D. W. Schmitz, *Ann. Rev. Nucl. Part. Sci.* **69**, 363 (2019), arXiv:1903.04608 [hep-ex].
- [8] A. Diaz, C. A. Argüelles, G. H. Collin, J. M. Conrad, and M. H. Shaevitz, *Phys. Rept.* **884**, 1 (2020), arXiv:1906.00045 [hep-ex].
- [9] C. A. Argüelles *et al.*, *Rept. Prog. Phys.* **83**, 124201 (2020), arXiv:1907.08311 [hep-ph].
- [10] P. Adamson *et al.* (MINOS+), *Phys. Rev. Lett.* **122**, 091803 (2019), arXiv:1710.06488 [hep-ex].
- [11] M. G. Aartsen *et al.* (IceCube), *Phys. Rev. Lett.* **125**, 141801 (2020), arXiv:2005.12942 [hep-ex].
- [12] M. Dentler, A. Hernández-Cabezudo, J. Kopp, P. A. N. Machado, M. Maltoni, I. Martinez-Soler, and T. Schwetz, *JHEP* **08**, 010 (2018), arXiv:1803.10661 [hep-ph].
- [13] C. Giunti, Y. F. Li, and Y. Y. Zhang, *JHEP* **05**, 061 (2020), arXiv:1912.12956 [hep-ph].
- [14] M. Aker *et al.* (KATRIN), *Phys. Rev. Lett.* **123**, 221802 (2019), arXiv:1909.06048 [hep-ex].
- [15] S. Dodelson and L. M. Widrow, *Phys. Rev. Lett.* **72**, 17 (1994), arXiv:hep-ph/9303287.
- [16] E. Bulbul, M. Markevitch, A. Foster, R. K. Smith, M. Loewenstein, and S. W. Randall, *Astrophys. J.* **789**, 13 (2014), arXiv:1402.2301 [astro-ph.CO].
- [17] A. Boyarsky, O. Ruchayskiy, D. Iakubovskiy, and J. Franse, *Phys. Rev. Lett.* **113**, 251301 (2014), arXiv:1402.4119 [astro-ph.CO].
- [18] C. Dessert, N. L. Rodd, and B. R. Safdi, *Science* **367**, 1465 (2020), arXiv:1812.06976 [astro-ph.CO].
- [19] F. Hofmann and C. Wegg, *Astron. Astrophys.* **625**, L7 (2019), arXiv:1905.00916 [astro-ph.HE].
- [20] B. M. Roach, K. C. Y. Ng, K. Perez, J. F. Beacom, S. Horiuchi, R. Krivonos, and D. R. Wik, *Phys. Rev. D* **101**, 103011 (2020), arXiv:1908.09037 [astro-ph.HE].
- [21] A. Caputo, M. Regis, and M. Taoso, *JCAP* **03**, 001 (2020), arXiv:1911.09120 [astro-ph.CO].
- [22] S. Bhargava *et al.*, *Mon. Not. Roy. Astron. Soc.* **497**, 656 (2020), arXiv:2006.13955 [astro-ph.CO].
- [23] E. M. Silich, K. Jahoda, L. Angelini, P. Kaaret, A. Zaczek, D. M. LaRocca, R. Ringueite, and J. Richardson, *Astrophys. J.* **916**, 2 (2021), arXiv:2105.12252 [astro-ph.HE].
- [24] C. A. Argüelles, V. Brdar, and J. Kopp, *Phys. Rev. D* **99**, 043012 (2019), arXiv:1605.00654 [hep-ph].
- [25] A. M. Suliga, I. Tamborra, and M.-R. Wu, *JCAP* **08**, 018 (2020), arXiv:2004.11389 [astro-ph.HE].
- [26] S. Hagstotz, P. F. de Salas, S. Gariazzo, M. Gerbino, M. Lattanzi, S. Vagnozzi, K. Freese, and S. Pastor, (2020), arXiv:2003.02289 [astro-ph.CO].
- [27] N. Aghanim *et al.* (Planck), *Astron. Astrophys.* **641**, A6 (2020), [Erratum: *Astron. Astrophys.* 652, C4 (2021)], arXiv:1807.06209 [astro-ph.CO].
- [28] A. G. Riess, S. Casertano, W. Yuan, L. M. Macri, and D. Scolnic, *Astrophys. J.* **876**, 85 (2019), arXiv:1903.07603 [astro-ph.CO].
- [29] C. D. Kreisch, F.-Y. Cyr-Racine, and O. Doré, *Phys. Rev. D* **101**, 123505 (2020), arXiv:1902.00534 [astro-ph.CO].
- [30] S. Hannestad, R. S. Hansen, and T. Tram, *Phys. Rev. Lett.* **112**, 031802 (2014), arXiv:1310.5926 [astro-ph.CO].
- [31] B. Dasgupta and J. Kopp, *Phys. Rev. Lett.* **112**, 031803 (2014), arXiv:1310.6337 [hep-ph].
- [32] A. Mirizzi, G. Mangano, O. Pisanti, and N. Saviano, *Phys. Rev. D* **91**, 025019 (2015), arXiv:1410.1385 [hep-ph].
- [33] N. Saviano, O. Pisanti, G. Mangano, and A. Mirizzi, *Phys. Rev. D* **90**, 113009 (2014), arXiv:1409.1680 [astro-ph.CO].
- [34] X. Chu, B. Dasgupta, and J. Kopp, *JCAP* **10**, 011 (2015), arXiv:1505.02795 [hep-ph].
- [35] L. Vecchi, *Phys. Rev. D* **94**, 113015 (2016), arXiv:1607.04161 [hep-ph].
- [36] F. Capozzi, I. M. Shoemaker, and L. Vecchi, *JCAP* **07**, 021 (2017), arXiv:1702.08464 [hep-ph].
- [37] N. Song, M. C. Gonzalez-Garcia, and J. Salvado, *JCAP* **10**, 055 (2018), arXiv:1805.08218 [astro-ph.CO].
- [38] P. Abratenko *et al.* (MicroBooNE), (2021), arXiv:2110.14054 [hep-ex].
- [39] P. Abratenko *et al.* (MicroBooNE), (2021), arXiv:2110.14080 [hep-ex].
- [40] P. Abratenko *et al.* (MicroBooNE), (2021), arXiv:2110.14065 [hep-ex].
- [41] P. Abratenko *et al.* (MicroBooNE), (2021), arXiv:2110.13978 [hep-ex].
- [42] J. Liao and D. Marfatia, *Phys. Rev. Lett.* **117**, 071802 (2016), arXiv:1602.08766 [hep-ph].
- [43] P. B. Denton, Y. Farzan, and I. M. Shoemaker, *Phys. Rev. D* **99**, 035003 (2019), arXiv:1811.01310 [hep-ph].
- [44] S. N. Gninenko, *Phys. Rev. D* **83**, 015015 (2011), arXiv:1009.5536 [hep-ph].
- [45] L. Alvarez-Ruso and E. Saul-Sala, in *Prospects in Neutrino Physics* (2017) arXiv:1705.00353 [hep-ph].
- [46] J. Asadi, E. Church, R. Guenette, B. J. P. Jones, and A. M. Szec, *Phys. Rev. D* **97**, 075021 (2018), arXiv:1712.08019 [hep-ph].
- [47] P. Ballett, S. Pascoli, and M. Ross-Lonergan, *Phys. Rev. D* **99**, 071701 (2019), arXiv:1808.02915 [hep-ph].
- [48] J. R. Jordan, Y. Kahn, G. Krnjaic, M. Moschella, and J. Spitz, *Phys. Rev. Lett.* **122**, 081801 (2019), arXiv:1810.07185 [hep-ph].
- [49] E. Bertuzzo, S. Jana, P. A. N. Machado, and R. Zukanovich Funchal, *Phys. Rev. Lett.* **121**, 241801 (2018), arXiv:1807.09877 [hep-ph].
- [50] O. Fischer, A. Hernández-Cabezudo, and T. Schwetz, *Phys. Rev. D* **101**, 075045 (2020), arXiv:1909.09561 [hep-ph].
- [51] A. Abdullahi, M. Hostert, and S. Pascoli, *Phys. Lett. B* **820**, 136531 (2021), arXiv:2007.11813 [hep-ph].
- [52] B. Dutta, S. Ghosh, and T. Li, *Phys. Rev. D* **102**, 055017

- (2020), [arXiv:2006.01319 \[hep-ph\]](#).
- [53] W. Abdallah, R. Gandhi, and S. Roy, *Phys. Rev. D* **104**, 055028 (2021), [arXiv:2010.06159 \[hep-ph\]](#).
- [54] S. Vergani, N. W. Kamp, A. Diaz, C. A. Argüelles, J. M. Conrad, M. H. Shaevitz, and M. A. Uchida, *Phys. Rev. D* **104**, 095005 (2021), [arXiv:2105.06470 \[hep-ph\]](#).
- [55] M. Antonello *et al.* (MicroBooNE, LAr1-ND, ICARUS-WA104), (2015), [arXiv:1503.01520 \[physics.ins-det\]](#).
- [56] G. J. Feldman and R. D. Cousins, *Phys. Rev. D* **57**, 3873 (1998), [arXiv:physics/9711021](#).
- [57] J. M. Berryman and P. Huber, *JHEP* **01**, 167 (2021), [arXiv:2005.01756 \[hep-ph\]](#).
- [58] K. Goldhagen, M. Maltoni, S. Reichard, and T. Schwetz, (2021), [arXiv:2109.14898 \[hep-ph\]](#).
- [59] J. N. Abdurashitov *et al.* (SAGE), *Phys. Rev. C* **80**, 015807 (2009), [arXiv:0901.2200 \[nucl-ex\]](#).
- [60] F. Kaether, W. Hampel, G. Heusser, J. Kiko, and T. Kirsten, *Phys. Lett. B* **685**, 47 (2010), [arXiv:1001.2731 \[hep-ex\]](#).
- [61] C. Giunti, M. Laveder, Y. F. Li, Q. Y. Liu, and H. W. Long, *Phys. Rev. D* **86**, 113014 (2012), [arXiv:1210.5715 \[hep-ph\]](#).
- [62] J. Kostensalo, J. Suhonen, C. Giunti, and P. C. Srivastava, *Phys. Lett. B* **795**, 542 (2019), [arXiv:1906.10980 \[nucl-th\]](#).
- [63] C. Giunti, X. P. Ji, M. Laveder, Y. F. Li, and B. R. Littlejohn, *JHEP* **10**, 143 (2017), [arXiv:1708.01133 \[hep-ph\]](#).
- [64] C. Giunti, Y. F. Li, B. R. Littlejohn, and P. T. Surukuchi, *Phys. Rev. D* **99**, 073005 (2019), [arXiv:1901.01807 \[hep-ph\]](#).
- [65] M. Andriamirado *et al.* (PROSPECT), *Phys. Rev. D* **103**, 032001 (2021), [arXiv:2006.11210 \[hep-ex\]](#).
- [66] C. Giunti, Y. F. Li, C. A. Ternes, and Z. Xin, (2021), [arXiv:2110.06820 \[hep-ph\]](#).
- [67] F. P. An *et al.* (Daya Bay), *Phys. Rev. Lett.* **118**, 251801 (2017), [arXiv:1704.01082 \[hep-ex\]](#).
- [68] D. Adey *et al.* (Daya Bay), *Phys. Rev. Lett.* **123**, 111801 (2019), [arXiv:1904.07812 \[hep-ex\]](#).
- [69] G. Bak *et al.* (RENO), *Phys. Rev. Lett.* **122**, 232501 (2019), [arXiv:1806.00574 \[hep-ex\]](#).
- [70] F. P. An *et al.*, (2021), [arXiv:2106.12251 \[nucl-ex\]](#).
- [71] T. A. Mueller *et al.*, *Phys. Rev. C* **83**, 054615 (2011), [arXiv:1101.2663 \[hep-ex\]](#).
- [72] P. Huber, *Phys. Rev. C* **84**, 024617 (2011), [Erratum: *Phys. Rev. C* **85**, 029901 (2012)], [arXiv:1106.0687 \[hep-ph\]](#).
- [73] L. Hayen, J. Kostensalo, N. Severijns, and J. Suhonen, *Phys. Rev. C* **100**, 054323 (2019), [arXiv:1908.08302 \[nucl-th\]](#).
- [74] M. Estienne *et al.*, *Phys. Rev. Lett.* **123**, 022502 (2019), [arXiv:1904.09358 \[nucl-ex\]](#).
- [75] V. Kopeikin, M. Skorokhvatov, and O. Titov, *Phys. Rev. D* **104**, L071301 (2021), [arXiv:2103.01684 \[nucl-ex\]](#).
- [76] S. Parke and M. Ross-Lonergan, *Phys. Rev. D* **93**, 113009 (2016), [arXiv:1508.05095 \[hep-ph\]](#).
- [77] S. A. R. Ellis, K. J. Kelly, and S. W. Li, *JHEP* **12**, 068 (2020), [arXiv:2008.01088 \[hep-ph\]](#).
- [78] Z. Hu, J. Ling, J. Tang, and T. Wang, *JHEP* **01**, 124 (2021), [arXiv:2008.09730 \[hep-ph\]](#).
- [79] G. Van Rossum and F. L. Drake, *Python 3 Reference Manual* (CreateSpace, Scotts Valley, CA, 2009).
- [80] J. D. Hunter, *Computing in Science & Engineering* **9**, 90 (2007).
- [81] X. Qian (MicroBooNE), “Search for an Anomalous Excess in Neutrino-Induced Interactions in the MicroBooNE Liquid Argon Time Projection Chamber,” BNL Colloquium (2021).